Science Advances
AAAS

advances.sciencemag.org/cgi/content/full/7/13/eabc6345/DC1

Supplementary Materials for

A cryo–electron tomography workflow reveals protrusion-mediated shedding on injured plasma membrane

Shrawan Kumar Mageswaran, Wei Yuan Yang*, Yogaditya Chakrabarty, Catherine M. Oikonomou, Grant J. Jensen*

*Corresponding author. Email: jensen@caltech.edu (G.J.J.); weiyang@gate.sinica.edu.tw (W.Y.Y.)

Published 26 March 2021, *Sci. Adv.* **7**, eabc6345 (2021)
DOI: 10.1126/sciadv.abc6345

The PDF file includes:

Other Supplementary Material for this manuscript includes the following:

(available at advances.sciencemag.org/cgi/content/full/7/13/eabc6345/DC1)

1. Supplementary Figures

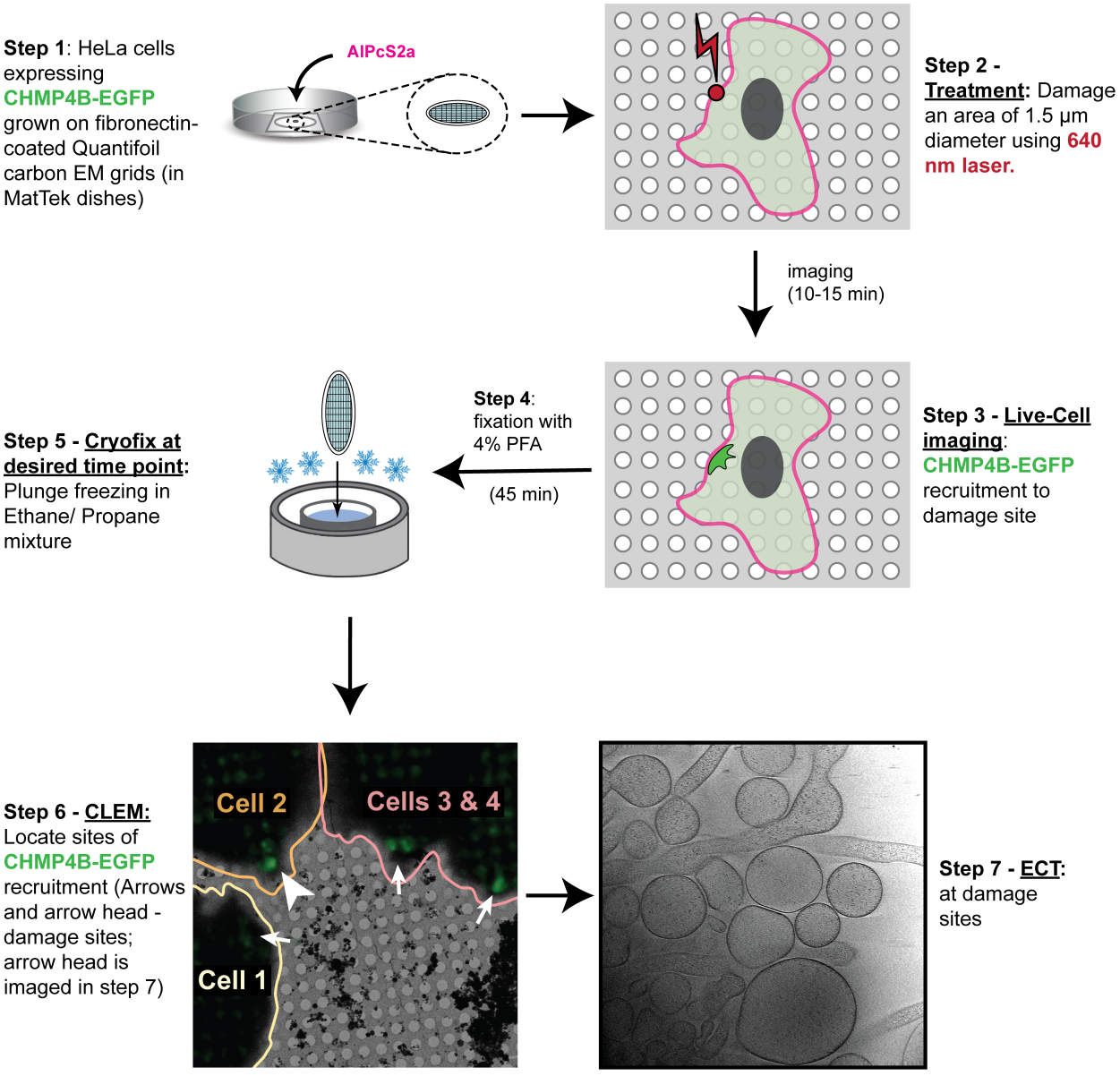

Fig. S1: Schematic for the experimental CLEM workflow.

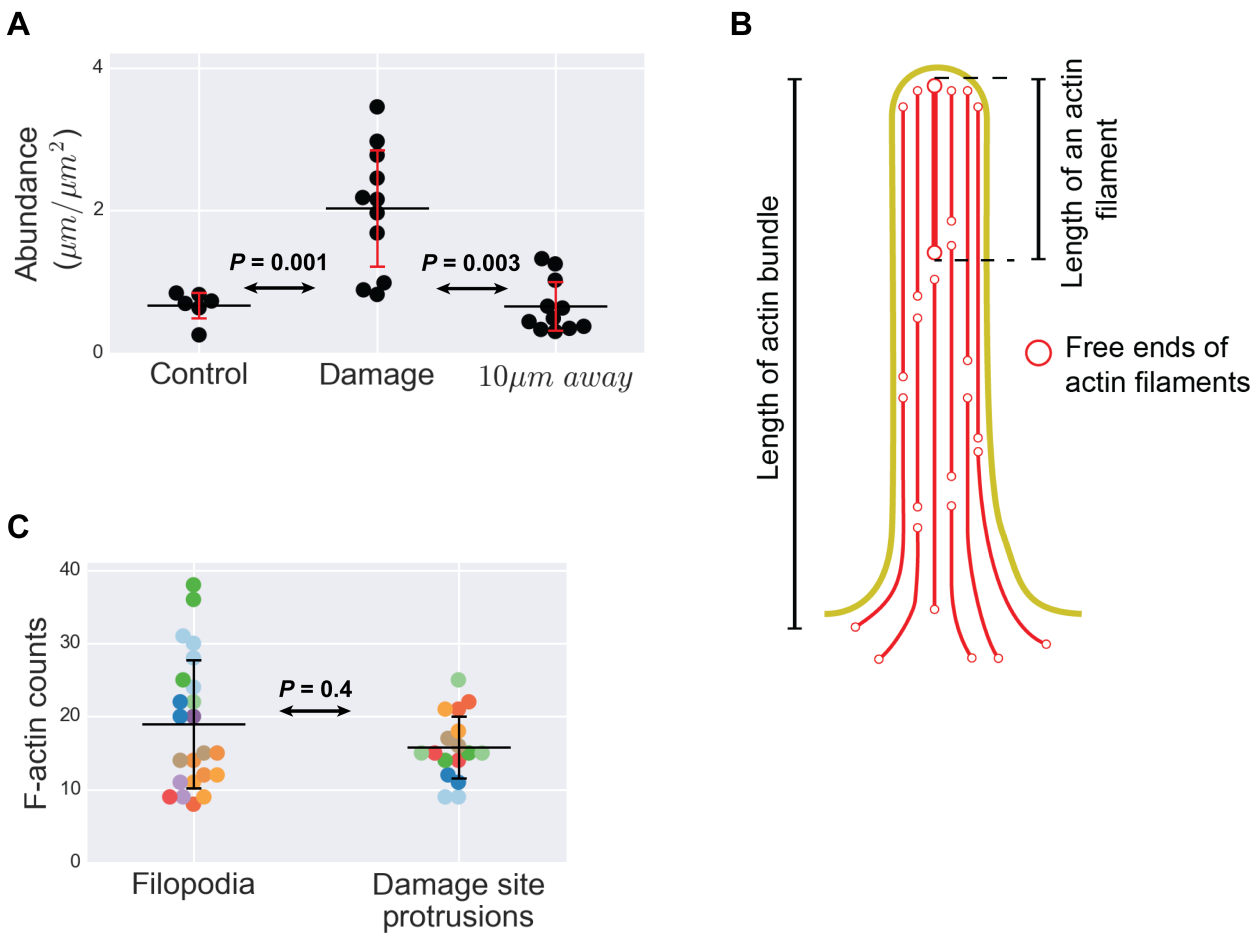

Fig. S2: CryoEM analysis of plasma membrane protrusions and their F-actin organization.

(A) Abundance (micrometers of protrusions per square micrometer cross-sectional area) at damage sites (n = 11), regions ~10 μm away from these damage sites (n = 11) and in control sites randomly chosen from undamaged cells (n = 6). Horizontal lines denote the mean values while the vertical red error bars denote SD (±1 SD) for each distribution. Projection images were used for this quantification. (B) Schematic for F-actin architecture within filopodia and damage site protrusions. (C) F-actin counts along the length of plasma membrane protrusions. Points of the same color denote measurements obtained on the same protrusion at different positions along its length. Horizontal lines denote the mean values while the vertical error bars denote SD

(±1 SD) for each distribution. Twenty-three measurements were made on 11 filopodia (from 3 tomograms) and 17 measurements on 8 damage site protrusions (from 4 tomograms).

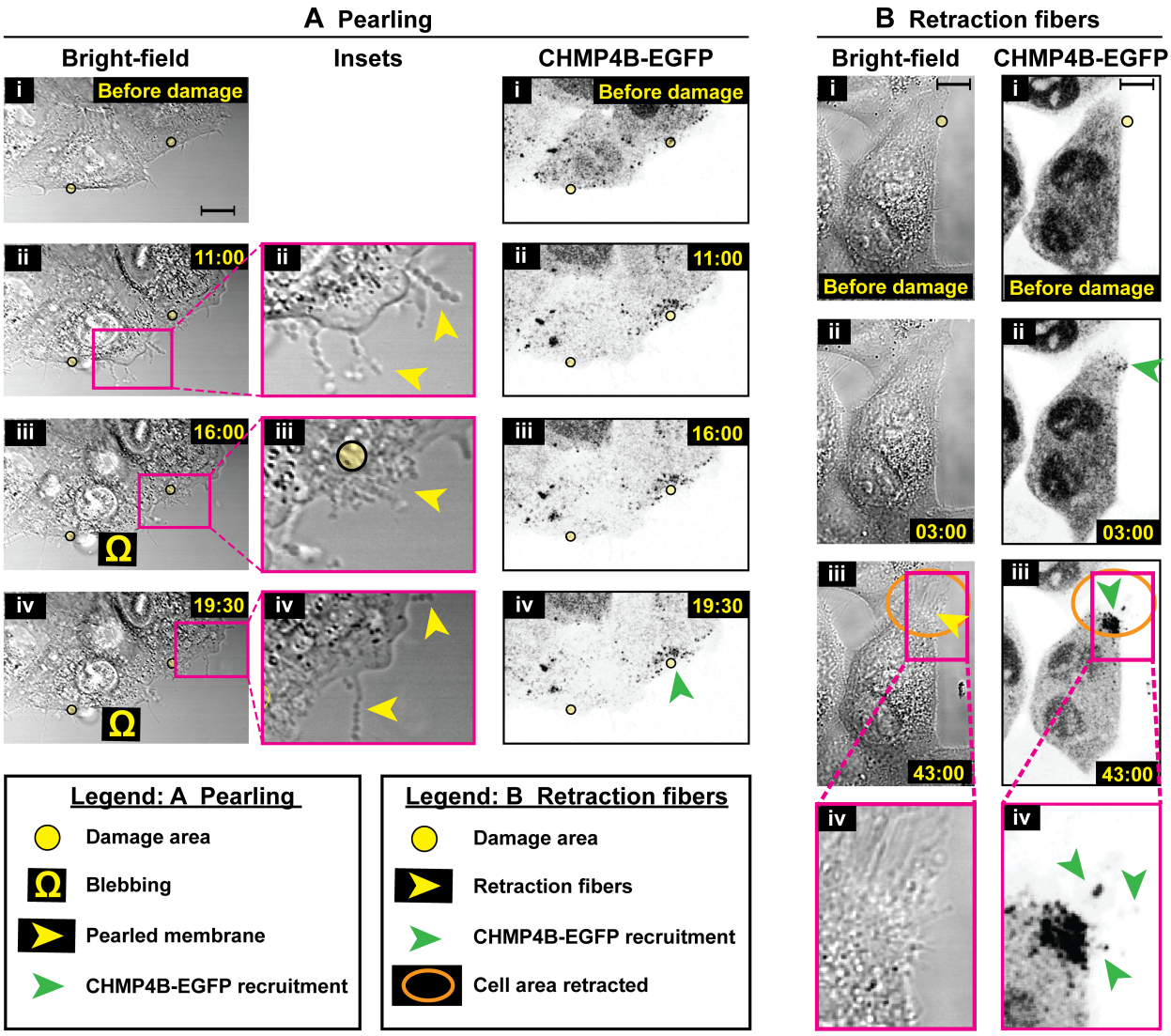

Fig. S3: Live-cell light microscopy of plasma membrane damage sites showing pearling and retraction fibers.

(A) Light microscopy images of HeLa cells grown on glass (i) before and (ii to iv) at various time points after damage showing membrane pearling – (left) bright-field images, (middle) magnified images of insets in the left panels, and (right) CHMP4B-EGFP images. (B) Light microscopy images of HeLa cells grown on glass (i) before and (ii to iii) at various time points after damage – (left) bright-field images showing retraction fibers, and (right) CHMP4B-EGFP images showing its recruitment to the retraction fibers. EGFP fluorescence is shown using inverted gray scale. The damage areas are 3 µm in diameter. Scale bars, 10 µm.

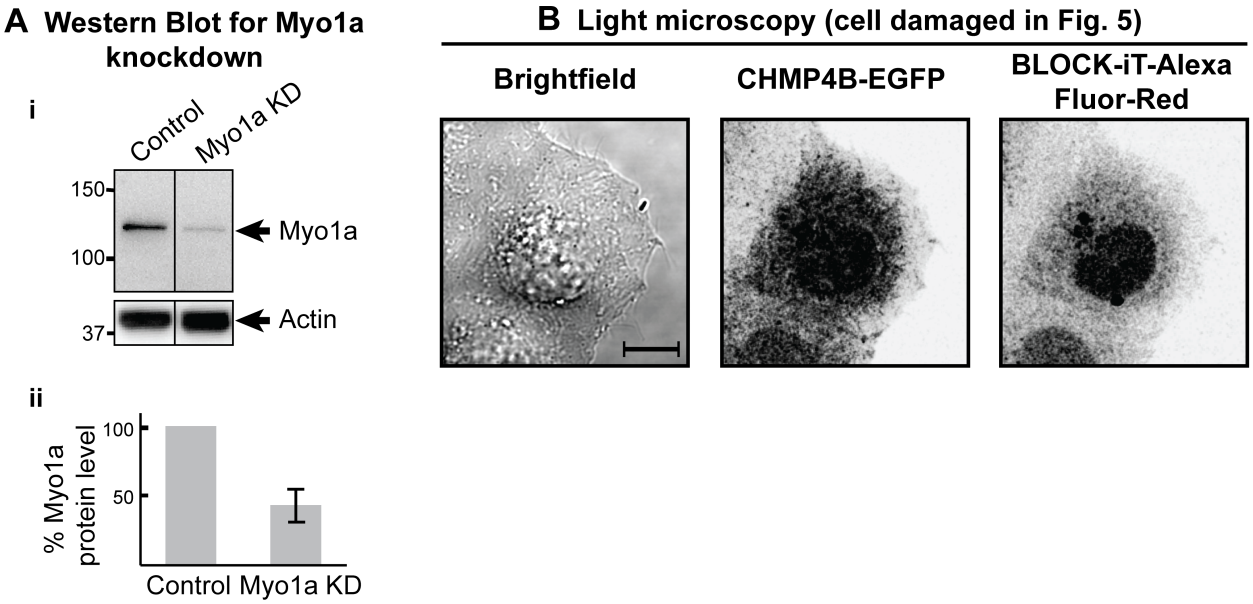

Fig. S4: Efficiency of siRNA transfection and Myo1a knockdown.

(A) (i) Western blot showing the protein levels of Myo1a upon siRNA-mediated knockdown compared to control siRNA transfected cells. Actin serves as the loading control. (ii) Quantification of Myo1a protein levels from three different knockdown experiments relative to control siRNA transfection experiments and normalized using actin loading control. SD values (±1 SD) are shown as error bars. (B) Light microscopy images of damaged cell in Fig. 5a – (left) bright-field image, (middle) CHMP4B-EGFP expression, and (right) BLOCK-iT-AlexaFluor-Red control RNA; the latter is used as a readout for transfection efficiency. EGFP and AlexaFluor-Red fluorescence are shown using inverted gray scale. Scale bars, 10 μm (B).

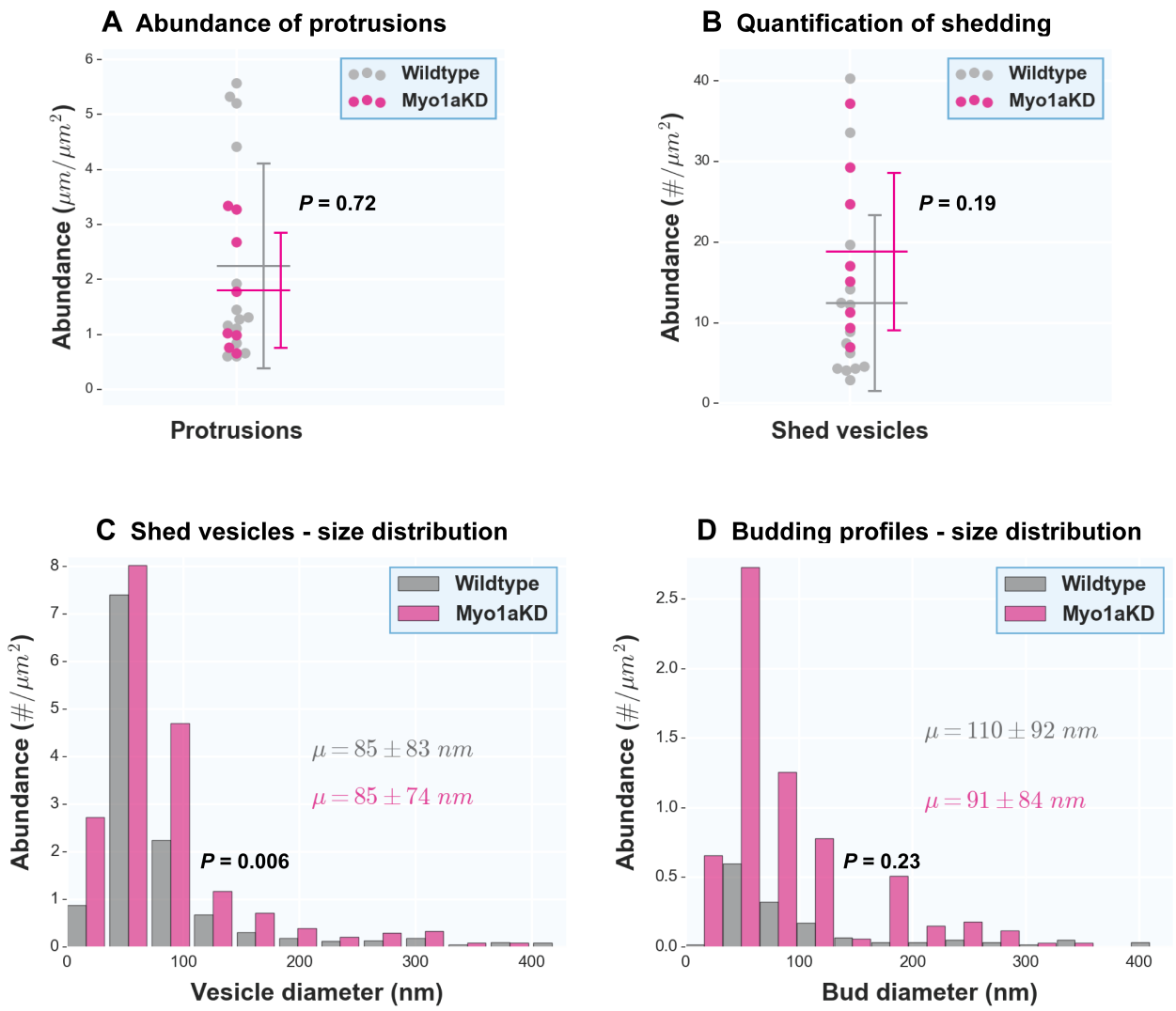

Fig. S5: Damage response in Myo1a knockdown cells by cryo-ET.

(A) Quantification of plasma membrane protrusions at damage sites of Myo1a knockdown cells versus wildtype (total length of protrusions in micrometers per square micrometer tomogram X-Y cross-sectional area). (B) Quantification of shed vesicles at damage sites of Myo1a knockdown cells versus wildtype (number of vesicles per square micrometer tomogram X-Y cross-sectional area). (C) Size distribution of shed vesicles at damage sites of Myo1a knockdown cells versus wildtype (no of vesicles in each size range per square micrometer tomogram X-Y cross-sectional area) along with their mean ± SD values. (D) Size distribution of budding profiles at damage sites of Myo1a knockdown cells versus wildtype (number of budding

profiles in each size range per square micrometer tomogram X-Y cross-sectional area) along with their mean ± SD values. In (A) and (B), each data point represents a tomogram. Horizontal lines denote the mean values while the vertical error bars denote SD (±1 SD) for each distribution. *P* values for pairwise comparison of distributions are obtained using KS tests. Sample sizes for quantifications: 8 tomograms for Myo1a knockdown (versus 10 tomograms for wildtype).

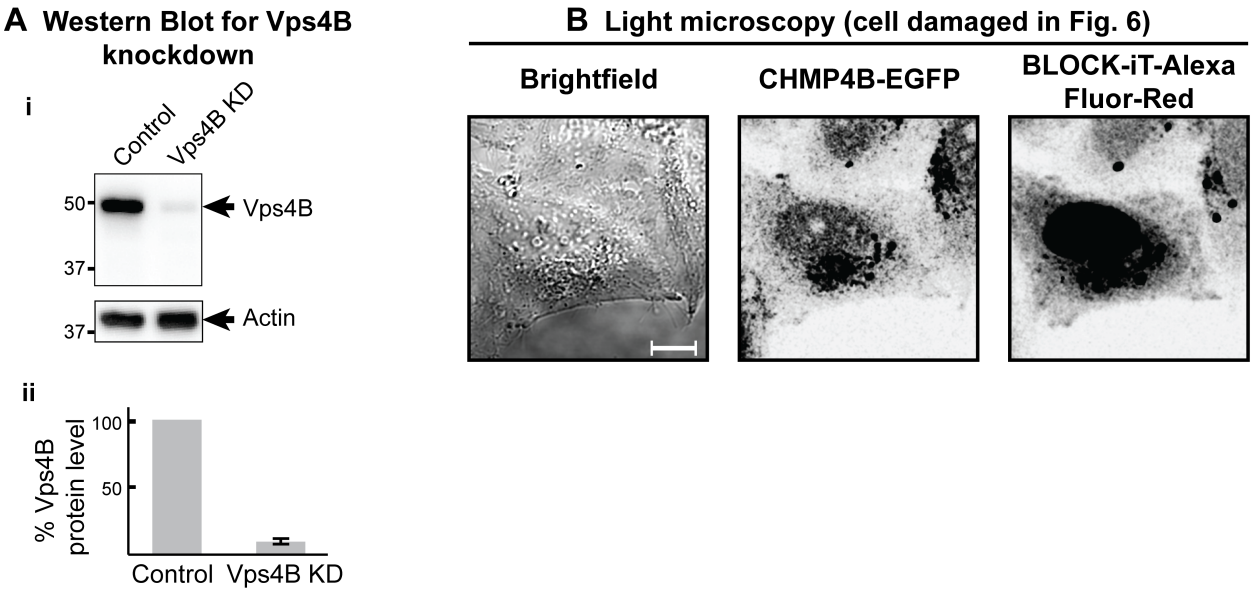

Fig. S6: Efficiency of siRNA transfection and Vps4B knockdown.

(A) (i) Western blot showing a reduction in the protein levels of Vps4B upon siRNA-mediated knockdown compared to control siRNA transfected cells. Actin serves as the loading control. (ii) Quantification of Vps4B protein levels from three different knockdown experiments relative to control siRNA transfection experiments and normalized using actin loading control. SD values (±1 SD) are shown as error bars. (B) Light microscopy images of damaged cell in Fig. 6a – (left) bright-field image, (middle) CHMP4B-EGFP expression, and (right) BLOCK-iT-AlexaFluor-Red control RNA; the latter is used as a readout for transfection efficiency. EGFP and AlexaFluor-Red fluorescence are shown using inverted gray scale. Scale bars, 10 μm (B).

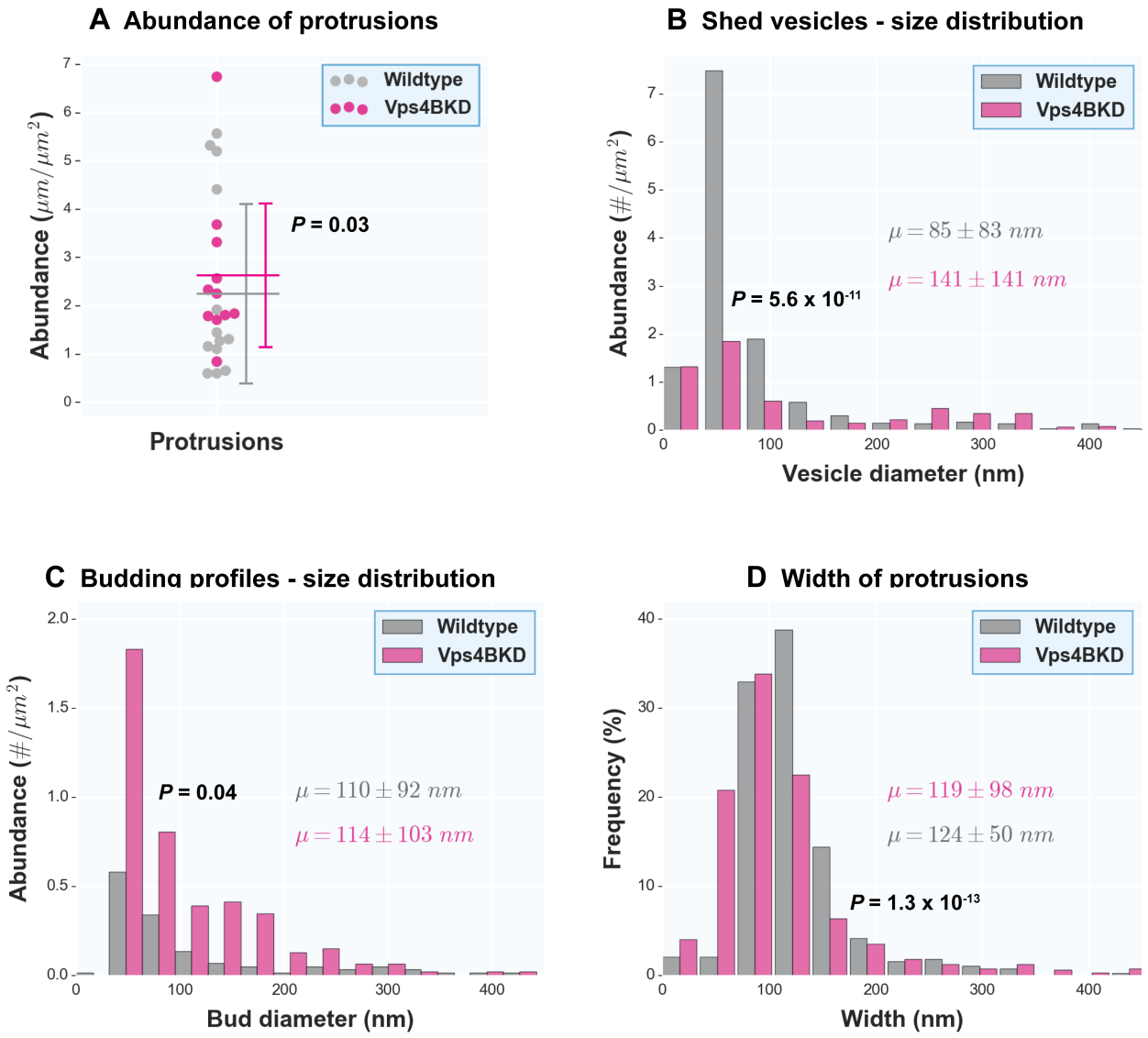

Fig. S7: Damage response in Vps4B knockdown cells by cryo-ET.

(A) Quantification of plasma membrane protrusions at damage sites of Vps4B knockdown cells versus wildtype (total length of protrusions in micrometers per square micrometer tomogram X-Y cross-sectional area). Each data point represents a tomogram. Horizontal lines denote the mean values while the vertical error bars denote SD (±1 SD) for each distribution. The means of the two distributions (although marginally and significantly different) are very similar (~2.5 µm of protrusions per square micrometer tomogram X-Y cross-sectional area). (B) Size distribution of shed vesicles at damage sites of Vps4B knockdown cells versus wildtype (number of vesicles in

each size range per square micrometer tomogram X-Y cross-sectional area) along with their mean ± SD values. (C) Size distribution of budding profiles at damage sites of Vps4B knockdown cells versus wildtype (number of buds in each size range per square micrometer tomogram X-Y cross-sectional area) along with their mean ± SD values. (D) Width distribution of protrusions at damage sites of Vps4B knockdown cells versus wildtype (percentage in each size range) along with their mean ± SD values. *P* values for pairwise comparison of distributions are obtained using KS tests. Sample sizes for quantifications: 11 tomograms for Vps4B knockdown (versus 10 tomograms for wildtype).

2. Supplementary Movies

Movie S1: Representative experiment including CLEM, cryo-ET and segmentation of a damage site. 00:00 – 00:18: Cells expressing CHMP4B-EGFP (green) were grown on R2/2 quantifoil grids (200 mesh London finder) in which the holes are 2 µm in diameter and spaced 2 µm apart from each other. 00:19 – 00:30: Cells were subjected to laser damage in an area of 1.5 µm in diameter resulting in CHMP4B-EGFP recruitment at and around these sites. 00:31 – 00:47: CLEM for damage sites 1 and 2. 00:48 – 03:18: Damage site 1. 00:56 – 01:03: Cryo-ET. 01:04 – 01:15: Segmentation of F-actin (red), plasma membrane (along with budding profiles; yellow), external membranes (free vesicles; green), internal membranes (cyan), and protein densities lining the inner surfaces of membranes at high curvature both in free vesicles and budding profiles (light magenta). 01:36 – 01:50 and 02:21 – 02:41: Plasma membrane protrusions. 01:51 – 02:14: Budding profiles. 02:50 – 03:05: Shed vesicles. 03:19 – 05:57: Damage site 2. 03:31 – 03:37: Cryo-ET. 03:38 – 03:48: Segmentation (same colors as damage site 1). 04:04 – 05:03: Plasma membrane protrusions. 04:35 – 05:03: Pearling. 05:08 – 05:55: Shed vesicles.

Movie S2: Light microscopy of a laser-damaged cell showing FusionRed-Pls1 localization in both regular filopodia and damage-induced protrusions.
The damage area (yellow circle) is 3 µm in diameter and the time points after damage are denoted in minutes:seconds.

Movie S3: Live-cell light microscopy of laser-damaged cells (6 cells, including the one shown in Fig. 3). Cell 1: *00:00 – 00:07*; Cell 2: *00:08 – 01:10*; Cell 3: *01:11 – 02:23*; Cell 4: *02:24 – 03:32*; Cell 5: *03:33 – 04:24*; Cell 6: *04:25 – 05:22*.